

University of Wisconsin - Madison

MAD/PH/878

UB-HET-95-02

March 1995

Finite Width Effects and Gauge Invariance in Radiative W Production and Decay

U. Baur¹ and D. Zeppenfeld²

¹*Department of Physics, State University of New York, Buffalo, NY 14260*

²*Department of Physics, University of Wisconsin, Madison, WI 53706*

ABSTRACT

The naive implementation of finite width effects in processes involving unstable particles can violate gauge invariance. For the example of radiative W production and decay, $q\bar{q}' \rightarrow \ell\nu\gamma$, at tree level, it is demonstrated how gauge invariance is restored by including the imaginary part of triangle graphs in addition to re-summing the imaginary contributions to the W vacuum polarization. Monte Carlo results are presented for the Fermilab Tevatron.

Radiative W boson production and decay at hadron colliders, *i.e.* the process $q\bar{q}' \rightarrow \ell^\pm \nu \gamma$, is an important testing ground for the Standard Model (SM). At large photon transverse momentum this process allows the measurement of the $WW\gamma$ three gauge boson coupling [1,2]. At small transverse momenta of the photon or when the photon is emitted collinearly to the final state charged lepton this process needs to be fully understood when trying to extract precise values of the W boson mass and width from the Tevatron data: in the CDF detector, for example, photon emission effects in W decays lead to a W mass shift of -65 ± 20 MeV (-168 ± 20 MeV) in the $W \rightarrow e\nu_e$ ($W \rightarrow \mu\nu_\mu$) channel [3], and a shift in the W width of 70 ± 28 MeV [4]. However, initial state radiation diagrams are not included in the Monte Carlo program currently used to simulate these effects [3,4].

Thus, a calculation is needed which fully describes initial and final state radiation, which implements the effects of the lepton mass, and which incorporates the finite W decay width, Γ_W . Finite lepton masses mostly affect photon radiation in the collinear region. Finite W width effects, on the other hand, play an important role for large angle soft photon bremsstrahlung, where the radiative W decay diagrams and $W\gamma$ production graphs may interfere substantially. In Ref. [5], radiative W decays were considered, including a full treatment of lepton mass effects. Initial state radiation was not incorporated into this calculation. In Ref. [2], we have calculated initial and final state radiation effects. However, since we were interested in the measurement of the $WW\gamma$ coupling, our Monte Carlo program did not allow the simulation of collinear final state photon radiation and the implementation of finite W width effects was inadequate for soft photon emission.

Part of the problem can be traced to the difficulty of implementing finite W width effects while maintaining electromagnetic gauge invariance [6]. The full process $q\bar{q}' \rightarrow \ell^\pm \nu \gamma$ proceeds via Feynman graphs with one (initial and final state radiation) and two W propagators (photon emission from the W). Replacing the W propagator factors $1/(q^2 - m_W^2)$ by a Breit-Wigner form, $1/(q^2 - m_W^2 + im_W\Gamma_W)$, will disturb the gauge cancellations between the individual Feynman graphs and thus lead to an amplitude which is not electromagnetically gauge invariant when finite lepton mass effects are included. In addition, a constant imagi-

nary part in the inverse propagator is ad hoc: it results from fermion loop contributions to the W vacuum polarization and the imaginary part should vanish for space-like momentum transfers.

In this Letter we demonstrate how this problem is solved by including the imaginary part of $WW\gamma$ vertex corrections in addition to the resummation of the W vacuum polarization contributions. The resulting amplitudes respect electromagnetic gauge invariance, are valid for arbitrary lepton masses, combine both initial and final state radiation, exhibit good high energy behaviour, and the imaginary parts of the propagators are exactly as derived from the W vacuum polarization. Even though we are only considering radiative W production and decay here, our method can immediately be generalized to t -channel processes such as $e^+e^- \rightarrow e^+W^-\nu_e \rightarrow e^+\nu_e d\bar{u}$ [7,8]. We also present some numerical results of our Monte Carlo calculation.

The general structure is best understood by first considering the lower order process ($q\bar{q}' \rightarrow \ell^-\bar{\nu}$ to be specific) without photon emission. The corresponding Feynman graphs are shown in Fig. 1. Finite width effects are included in a tree level calculation by resumming the imaginary part of the W vacuum polarization. When neglecting the fermion masses in the loops of Fig. 1 the transverse part of the W vacuum polarization receives an imaginary contribution

$$Im \Pi_W^T(q^2) = \sum_f \frac{g^2}{48\pi} q^2 = q^2 \frac{\Gamma_W}{m_W}, \quad (1)$$

while the imaginary part of the longitudinal piece vanishes. In the unitary gauge the W propagator is thus given by

$$\begin{aligned} D_W^{\mu\nu}(q) &= \frac{-i}{q^2 - m_W^2 + iIm \Pi_W^T(q^2)} \left(g^{\mu\nu} - \frac{q^\mu q^\nu}{q^2} \right) + \frac{i}{m_W^2 - iIm \Pi_W^L(q^2)} \frac{q^\mu q^\nu}{q^2} \\ &= \frac{-i}{q^2 - m_W^2 + iq^2\gamma_W} \left(g^{\mu\nu} - \frac{q^\mu q^\nu}{m_W^2} (1 + i\gamma_W) \right), \end{aligned} \quad (2)$$

where we have used the abbreviation $\gamma_W = \Gamma_W/m_W$. Note that the W propagator has received a q^2 dependent effective width which actually would vanish in the space-like region.

Since here we are only interested in (virtual) W decays we do not include the corresponding step-function factor.

A gauge invariant expression for the amplitude of the process $q\bar{q}' \rightarrow \ell^- \bar{\nu} \gamma$ is obtained by attaching the final state photon in all possible ways to all charged particle propagators in the Feynman graphs of Fig. 1. This includes radiation off the two incoming quark lines, radiation off the final state charged lepton, and radiation off the W propagators. In addition, the photon must be attached to the charged fermions inside the W vacuum polarization loops, leading to the fermion triangle graphs of Fig. 2. Since we are only keeping the imaginary part of $\Pi_W^T(q^2)$, consistency requires including the imaginary part of the triangle graphs only. This imaginary part is obtained by cutting the triangle graphs into on-shell intermediate states in all possible ways, as shown in the figure.

The full set of Feynman graphs contributing to $q\bar{q}' \rightarrow \ell^- \bar{\nu} \gamma$ is depicted in Fig. 3. When attaching the photon in all possible ways to either one of the fermion loops or to one of the lowest order W propagators in all graphs of Fig. 1, the remaining sum over W vacuum polarization graphs restores the full W propagator of Eq. (2) on either side of the triangle graph or the $WW\gamma$ vertex. Hence, after resummation, one obtains the Feynman graph of Fig. 3c where the full $WW\gamma$ vertex is given by the sum of the lowest order vertex and the imaginary part of the triangle graphs, as defined in Fig. 2.

For the momentum flow shown in Fig. 2 the lowest order vertex is given by the familiar expression

$$-ie\Gamma_0^{\alpha\beta\mu} = -ie \left((q_1 + q_2)^\mu g^{\alpha\beta} - (q_1 + k)^\beta g^{\mu\alpha} + (k - q_2)^\alpha g^{\mu\beta} \right) . \quad (3)$$

Neglecting the masses of the fermions in the triangle graphs and dropping terms proportional to k^μ (which will be contracted with the photon polarization vector $\varepsilon^{*\mu}$ and hence vanish in the amplitude) the contributions from the four triangle graphs reduce to an extremely simple form. Each fermion doublet f , irrespective of its hypercharge, adds $i(g^2/48\pi)\Gamma_0$ to the lowest order $WW\gamma$ vertex Γ_0 . After summing over all fermion species, the lowest order vertex is thus replaced by

$$\Gamma^{\alpha\beta\mu} = \Gamma_0^{\alpha\beta\mu} \left(1 + \sum_f \frac{ig^2}{48\pi} \right) = \Gamma_0^{\alpha\beta\mu} \left(1 + i \frac{\Gamma_W}{m_W} \right) = \Gamma_0^{\alpha\beta\mu} (1 + i\gamma_W) . \quad (4)$$

This expression corresponds to the full $WW\gamma$ vertex which is represented by the hatched blobs in Figs. 2 and 3.

By construction, the resulting amplitude for the process $q\bar{q}' \rightarrow \ell^- \bar{\nu}\gamma$ should be gauge invariant. Indeed, gauge invariance of the full amplitude can be traced to the electromagnetic Ward identity [6]

$$k_\mu \Gamma_{\alpha\beta}{}^\mu = (iD_W)_{\alpha\beta}^{-1}(q_1) - (iD_W)_{\alpha\beta}^{-1}(q_2) . \quad (5)$$

Since

$$k_\mu \Gamma^{\alpha\beta\mu} = \left((q_1^2 g^{\alpha\beta} - q_1^\alpha q_1^\beta) - (q_2^2 g^{\alpha\beta} - q_2^\alpha q_2^\beta) \right) (1 + i\gamma_W) , \quad (6)$$

and

$$(iD_W)_{\alpha\beta}^{-1}(q) = \left(q^2 - m_W^2 + iq^2\gamma_W \right) \left(g_{\alpha\beta} - \frac{q_\alpha q_\beta}{q^2} \right) - m_W^2 \frac{q_\alpha q_\beta}{q^2} , \quad (7)$$

this Ward identity is satisfied for the W propagator and $WW\gamma$ vertex of Eqs. (2) and (4).

There are other ways to include finite width effects while restoring electromagnetic gauge invariance [7]. One possibility is to multiply the complete tree level amplitude by an overall factor $F(q^2) = (q^2 - m_W^2)/(q^2 - m_W^2 + im_W\Gamma_W)$ for each almost on-shell W propagator [9]. This procedure implements Breit-Wigner propagators in all resonant graphs but multiplies non-resonant contributions by an ad-hoc factor. This is phenomenologically acceptable if the non-resonant contributions are sub-leading. For $W\gamma$ production, however, the “non-resonant” graphs of Fig. 3a,b are dominant near threshold and multiplying them by the factor $F(\hat{s})$ decreases *e.g.* the soft photon emission cross section by 30% or more as compared to the correct treatment described above.

Electromagnetic gauge invariance is also obtained by dropping the triangle graph contributions and using a naive Breit Wigner propagator [6],

$$D_{W,\text{naive}}^{\mu\nu}(q) = \frac{-i}{q^2 - m_W^2 + im_W\Gamma_W} \left(g^{\mu\nu} - \frac{q^\mu q^\nu}{m_W^2 - im_W\Gamma_W} \right) . \quad (8)$$

However, this propagator does not correspond to a resummation of W vacuum polarization graphs, the imaginary part does not vanish in the space-like region, and the imaginary part of the W mass squared in the longitudinal piece of the propagator is entirely unphysical. On theoretical grounds this solution of the gauge-invariance problem must therefore be rejected, even though, for the problem at hand, numerical results are very similar to the full treatment including triangle graphs.

The modification of the lowest order $WW\gamma$ vertex in Eq. (4) looks like the introduction of anomalous couplings $g_1^\gamma = \kappa_\gamma = 1 + i\gamma_W$ and one may thus worry that the full amplitude will violate unitarity at large center of mass energies $\sqrt{\hat{s}}$. While indeed the vertex is modified, this modification is compensated by the effective \hat{s} -dependent width in the propagator. As compared to the expressions with a lowest order propagator, $1/(\hat{s} - m_W^2)$, which of course has good high energy behaviour, the overall effect is multiplication of the analog of the Feynman graph of Fig. 3c by a factor

$$G(\hat{s}) = \frac{\hat{s} - m_W^2}{\hat{s}(1 + i\gamma_W) - m_W^2} (1 + i\gamma_W) = 1 - \frac{i\Gamma_W m_W}{\hat{s} - m_W^2 + im_W \Gamma_W \frac{\hat{s}}{m_W^2}}. \quad (9)$$

Obviously, $G(\hat{s}) \rightarrow 1$ as $\hat{s} \rightarrow \infty$ and the high energy behaviour of our finite width amplitude is identical to the one of the naive tree level result for $W\gamma$ production. In fact, the contributions from the triangle graphs are crucial to compensate the bad high energy behaviour introduced by the q^2 -dependent width in Eq. (2).

What are the results of our implementation of finite width, fermion triangle, and lepton mass effects? In Table I we give the fraction of $W^\pm \rightarrow \ell^\pm \nu$ events ($\ell = e, \mu$) at the Tevatron ($p\bar{p}$ collisions at $\sqrt{s} = 1.8$ TeV) which contain a photon with a transverse energy $E_T(\gamma) > E_T^0(\gamma)$. We then compare our results with the expectation for final state radiation only (in the narrow W -width approximation), as in Ref. [5]. Specifically, we consider the phase space region

$$p_T(\ell) > 25 \text{ GeV}, \quad \not{p}_T > 25 \text{ GeV}, \quad |\eta(\ell)| < 1, \quad |\eta(\gamma)| < 3.6 \\ 65 \text{ GeV} < m_T^W < 100 \text{ GeV}, \quad (10)$$

where m_T^W denotes the transverse mass of the $\ell\nu$ system. The phase space region defined by Eq. (10) is very similar to that used by CDF [3] and DØ [10] to extract the W mass. We then vary the requirements on the minimum photon transverse energy, $E_T^0(\gamma)$, and the lepton photon separation, $\Delta R(\ell, \gamma)$. QCD corrections and structure function effects largely cancel in the cross section ratio considered. Finite lepton masses are seen to hardly influence large angle photon radiation whereas the inclusive rate for photon radiation in the electron channel is about a factor two larger than the result obtained for muons. Initial state photon radiation approximately triples the fraction of W boson events which contain a well isolated photon ($\Delta R(\ell, \gamma) > 0.7$). It increases the total number of $W \rightarrow e\nu$ ($W \rightarrow \mu\nu$) events which contain a photon by typically $\sim 10\%$ ($\sim 20\%$). The event fractions presented in Table I are insensitive to the maximum absolute lepton pseudorapidity, η_{\max} , in the range $\eta_{\max} = 0.6 \dots 1.2$.

Finally, we briefly comment on radiative Z production and decay, $q\bar{q} \rightarrow Z\gamma \rightarrow \ell^+\ell^-\gamma$ and $q\bar{q} \rightarrow Z \rightarrow \ell^+\ell^-\gamma$. Since only diagrams with one Z propagator contribute, the gauge invariance problems encountered in the W case when incorporating finite lepton masses do not arise here, and the calculation is straightforward. Using the results of Ref. [11], we have calculated radiative Z production and decay including finite lepton masses at hadron colliders. The fraction of Z boson events which contains a photon with $E_T(\gamma) > E_T^0(\gamma)$ is about a factor 2 larger than the corresponding number in the W case. For $\Delta R(\ell, \gamma) > 0.7$, initial state radiation approximately doubles the number of Z boson events with a photon.

ACKNOWLEDGMENTS

We would like to thank M. Demarteau, S. Errede and Y.-K. Kim for many stimulating discussions. This research was supported in part by the University of Wisconsin Research Committee with funds granted by the Wisconsin Alumni Research Foundation and in part by the U. S. Department of Energy under Grant No. DE-FG02-95ER40896.

REFERENCES

- [1] F. Abe *et al.* (CDF Collaboration), FERMILAB-Pub-94/236-E, to appear in Phys. Rev. Lett. and FERMILAB-Pub-94/244-E, to appear in Phys. Rev. **D**; J. Ellison (DØ Collaboration), FERMILAB-Conf-94/329-E, (November 1994), to appear in the Proceedings of the “*DPF’94 Conference*”, Albuquerque, NM, August 1994.
- [2] U. Baur and D. Zeppenfeld, Nucl. Phys. **B308**, 127 (1988).
- [3] F. Abe *et al.* (CDF Collaboration), FERMILAB-Pub-95/033-E (March 1995), submitted to Phys. Rev. **D**, and FERMILAB-Pub-95/035-E (March 1995), submitted to Phys. Rev. Lett.
- [4] F. Abe *et al.* (CDF Collaboration), Phys. Rev. Lett. **74**, 341 (1995).
- [5] F. A. Berends and R. Kleiss, Z. Phys. **C27**, 365 (1985); R. G. Wagner, Comp. Phys. Comm. **70**, 15 (1992).
- [6] See *e.g.* G. Lopez Castro, J.L.M. Lucio, and J. Pestieau, Mod. Phys. Lett. **A6**, 3679 (1991); M. Nowakowski and A. Pilaftsis, Z. Phys. **C60**, 121 (1993) and references therein.
- [7] A. Aeppli, F. Cuyper and G. J. van Oldenborgh, Phys. Lett. **B314**, 413 (1993).
- [8] Y. Kurihara, D. Perret-Gallix and Y. Shimizu, KEK-PREPRINT-94-150 (December 1994); C. G. Papadopoulos, preprint CERN-TH/95-46 (March 1995).
- [9] U. Baur, J. Vermaseren, and D. Zeppenfeld, Nucl. Phys. **B375**, 3 (1992).
- [10] C. K. Jung, FERMILAB-Conf-94/334-E (October 1994), to appear in the Proceedings of the the “*27th International Conference on High Energy Physics*”, Glasgow, Scotland, July 1994; M. Demarteau, private communication.
- [11] U. Baur and E.L. Berger, Phys. Rev. **D47**, 4889 (1993).

TABLES

TABLE I. Fraction of $W \rightarrow e\nu$ and $W \rightarrow \mu\nu$ events (in percent) at the Tevatron ($p\bar{p}$ collisions at $\sqrt{s} = 1.8$ TeV). We consider events in the phase space region of Eq. (10) which contain a photon with transverse energy $E_T(\gamma) > E_T^0(\gamma)$ for two different minimal separations between the charged lepton and the photon, $\Delta R(\ell, \gamma)$. The results obtained by considering final state radiation only (in the narrow W width approximation) are shown in brackets.

$E_T^0(\gamma)$	$W \rightarrow e\nu$		$W \rightarrow \mu\nu$	
	$\Delta R(e, \gamma) > 0$	$\Delta R(e, \gamma) > 0.7$	$\Delta R(\mu, \gamma) > 0$	$\Delta R(\mu, \gamma) > 0.7$
0.1	19.3 (17.5)	3.63 (1.31)	11.8 (9.8)	3.62 (1.32)
0.3	14.8 (13.5)	2.56 (0.95)	8.76 (7.37)	2.54 (0.95)
1	9.42 (8.63)	1.45 (0.57)	5.37 (4.62)	1.44 (0.56)
3	4.58 (4.14)	0.66 (0.24)	2.55 (2.14)	0.65 (0.24)
10	0.55 (0.36)	0.13 (0.01)	0.32 (0.17)	0.13 (0.01)
30	0.014 (-)	0.012 (-)	0.013 (-)	0.012 (-)

FIGURES

FIG. 1. Feynman graphs for the lowest order process $q\bar{q}' \rightarrow \ell^-\bar{\nu}$. The resummation of the imaginary part of the W vacuum polarization leads to the Breit-Wigner type W propagator of Eq. (2) which is represented by the shaded blob.

FIG. 2. Effective $WW\gamma$ vertex as needed in the tree level calculation of $W\gamma$ production. In addition to the lowest order vertex the imaginary parts of the fermion triangles must be included (see Eq. (4)).

FIG. 3. Feynman graphs for the process $q\bar{q}' \rightarrow \ell^-\bar{\nu}\gamma$. The shaded and hatched blobs indicate the full W propagators as defined in Fig. 1 and the full $WW\gamma$ vertex as given in Fig. 2, respectively.

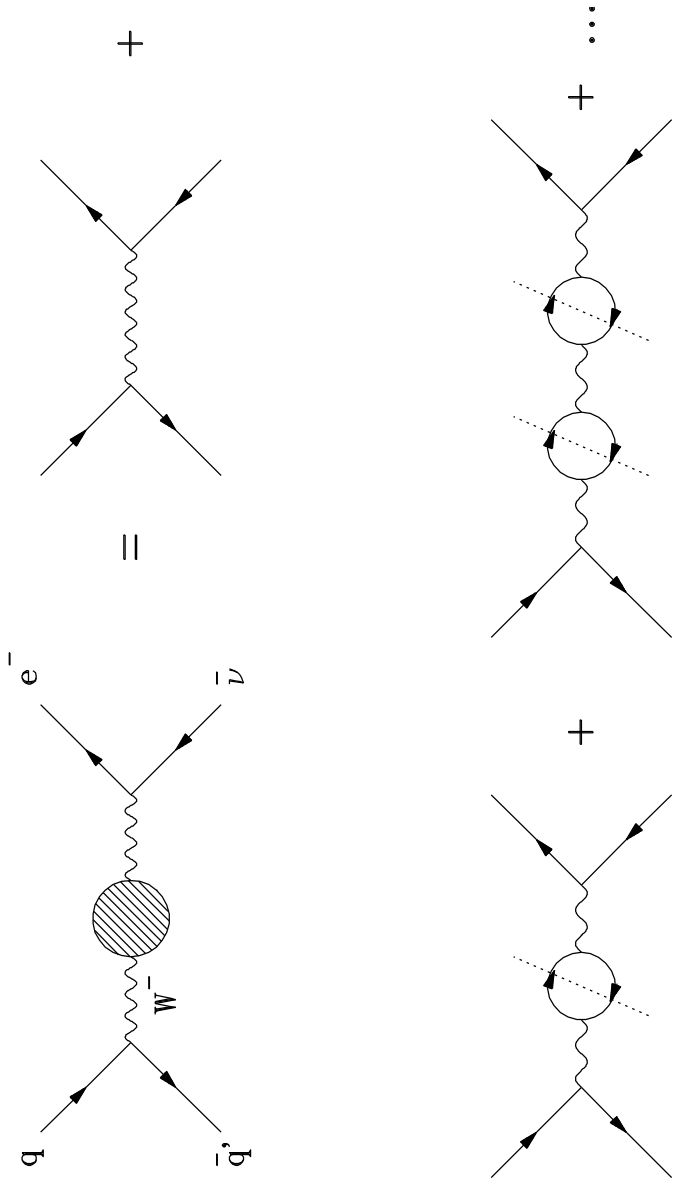


Figure 1

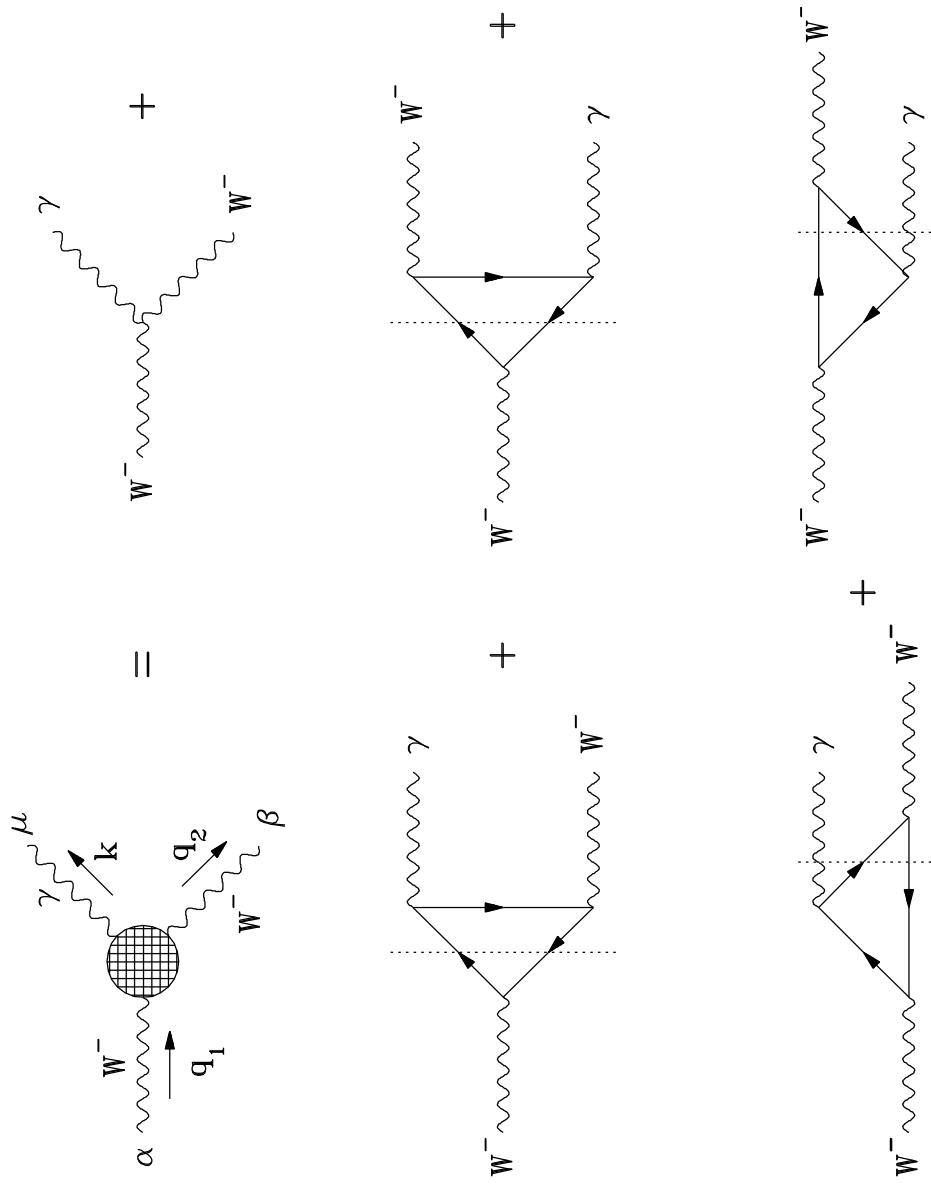


Figure 2

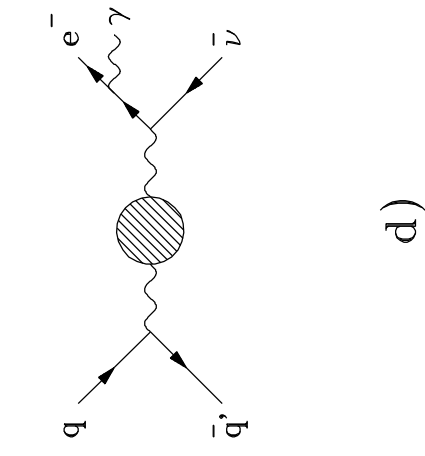
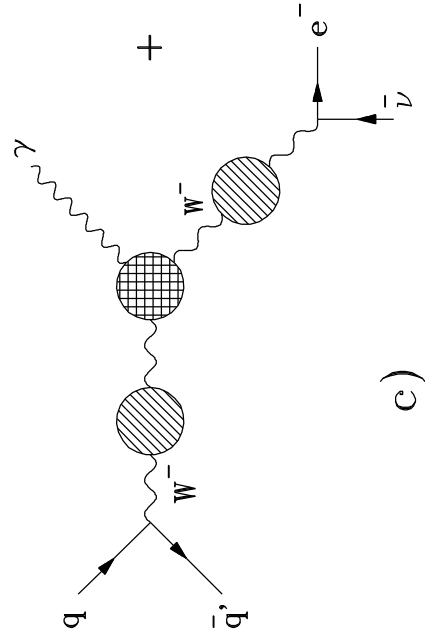
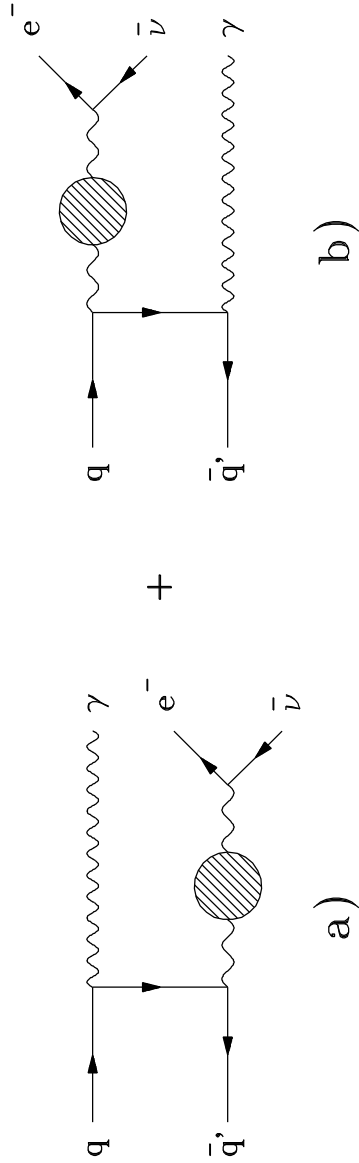


Figure 3